Sea-Tower Measurements of Wind-Wave Spectra in the Caspian Sea

I. A. LEYKIN AND A. D. ROZENBERG

P. P. Shirshov Institute of Oceanology, USSR Academy of Sciences, Moscow, 117218, USSR

(Manuscript received 17 July 1980, in final form 27 June 1983)

ABSTRACT

High frequency spectra of wind generated waves corresponding to mean wind speeds from 3.5 to 13.5 m s^{-1} were measured at the research tower in the Caspian Sea. The techniques used made it possible to evaluate spectra $S(\omega)$ in the frequency range extending to 10 Hz.

The data obtained clearly show that there is no equilibrium range in the high frequency part of the wind wave spectrum. The measured spectra within the frequency range from 2.4 to 7.2 Hz fit a power law, $S(\omega) = \alpha \cdot \omega^{-n}$, with the values of n changing from 3.2 to 4.8, and the values of the spectral density at the fixed frequency S_{ω_i} within this range were shown to increase with wind speed. The dependence of the shapes of the measured spectra on wind speed and the parameters of the long wave components is discussed.

A new expression for the wind-wave frequency spectrum $S(\omega)$ within the range $\omega > \omega_m$ (ω_m is the frequency of the spectral peak) is proposed based on the experimental data: it is expressed in terms of the difference between a particular frequency and the frequency of the spectral peak.

1. Introduction

In 1958 Phillips assumed the existence of a universal equilibrium range in the spectra of wind-generated gravity waves and suggested that the spectral density within this range is governed only by the parameters which characterize the wave breaking. According to Phillips (1958, 1977) for gravity waves the acceleration of gravity g is the only such parameter. Then on dimensional grounds one obtains the following expressions

$$S(\omega) = \beta g^2 \omega^{-5}, \tag{1}$$

$$\psi(\mathbf{K}) = Bk^{-4}\varphi(\theta), \tag{2}$$

where $S(\omega)$ and $\psi(\mathbf{K})$ are, respectively, the frequency and wavenumber spectra, ω the frequency, k the modulus of the wavenumber vector $\mathbf{K} = (k\cos\theta, k\sin\theta)$, θ the angle characterizing the direction of wave propagation, β and B are universal nondimensional constants and $\varphi(\theta)$ is an angular spreading factor.

The relation (1) described rather well all the data on the frequency spectra $S(\omega)$ which were available at that time. According to these data (Phillips, 1977) the constant β proved to be equal to 1.2×10^{-2}. It is important to stress that the frequency spectra $S(\omega)$ which were taken by Phillips to test the expression (1) included no high-frequency range ($\omega/2\pi \geq 2$ Hz).

For many years the relation (1) known as Phillips' spectrum was a widely used description of the high-frequency wave spectra and it is still widely used for description of wave spectra even though new data have revealed significant differences between observed spectra $S(\omega)$ and Eq. (1).

It has been shown that the value of the so-called "universal constant" β may change within the range of several orders. For example the data reported by Hasselmann *et al.* (1973) implied that the value of β decreases monotonically with nondimensional fetch $\hat{X} = gX/U^2$ (where U is the wind mean speed).

On the other hand, the approximation of observed spectra $S(\omega)$ by the function $S(\omega) = \alpha\omega^{-n}$ showed that the value of the shape parameter n may be significantly different from 5. According to Grose *et al.* (1972), who investigated the shape of the equilibrium range for 69 wind-wave spectra in the frequency range from 0.25 to 0.61 Hz, the values of n ranged between 2.5 and 4.3 with an average value of 3.6.

Analogous results were obtained by Yefimov and Kushnir (1974), who used the data of 24 spectra $S(\omega)$ measured in the coastal zone. The value of n in the frequency range from $1.2\omega_m$ to ω_h (where ω_m is the frequency of the spectral peak, and ω_h is the value of the highest frequency of the range under consideration, changing from $2\omega_m$ to $8\omega_m$ for different spectra) was found to lie between 3.8 and 5.3 with an average value of 4.36.

Other deviations from the law (1) were found as a result of measurements in the high-frequency spectral range ($\omega/2\pi \approx 1$–10 Hz), where the equilibrium range is more likely to be found. The pioneer measurements were undertaken by Leykin and Rozenberg (1970) in the coastal zone and showed no saturation range in the high-frequency range of the spectra $S(\omega)$ at least for wind speeds up to 10–12 m s^{-1}. The magnitude of spectral density at the fixed frequency S_{ω_i} was found to increase with wind speed and the spectral shapes fitted satisfactory an ω^{-4} power law.

These features of the high-frequency part of the spectra $S(\omega)$ were confirmed by further measurements (Mitsuyasu, 1977; Kondo *et al.*, 1973). However, the small number of high-frequency spectra reported by Mitsuyasu (1977) and Kondo *et al.* (1973) does not permit one to clarify the relation between spectrum $S(\omega)$ parameters and the wave generation conditions. Laboratory measurements have also shown an increase of the spectral density S_{ω_i} with the wind speed and the "ω^{-4}" power law for high-frequency spectra (Mitsuyasu and Honda, 1974; Toba, 1973). But these cannot be directly compared with the observations on larger bodies of water because under laboratory conditions there are no long wave components in wave spectra.

The long wave components corresponding to energy-containing components of wind waves or swell have a rather significant effect on the high-frequency part of the spectra $S(\omega)$ (Sinitsyn *et al.*, 1973; Zaslavskii and Kitaigorodskii, 1972; Phillips and Banner, 1974).

Taking into account the great importance of the high-frequency part of the wind wave spectra for our understanding of the remote sensing of the ocean surface, we have studied wind wave spectra $S(\omega)$ within the frequency range up to 10 Hz in the open sea. The primary purpose of these studies was to investigate the influence of long waves on the high-frequency part of the spectra $S(\omega)$.

2. Experimental facility and equipment

Wind waves were measured at a research sea tower located 10 miles northeast of Apsheron Peninsula in the open part of the Caspian Sea. The water depth at the tower is 40 m and the bottom around the tower is approximately flat with a gentle increase of depth in the north, east and south directions. The research tower is a rectangular platform (20 × 60 m) which is composed essentially of four vertical piles driven into the sea bottom. The tower has been designed mainly for wind and wave measurements in north winds. In order to minimize the distortions produced by the tower most of the equipment was located on the southern side of the platform while the wind and wave probes were concentrated at the northern (up-wind) side. A simplified sketch of the tower is shown in Fig. 1; a more detailed description of this tower was given earlier by Zubkovsky *et al.* (1974).

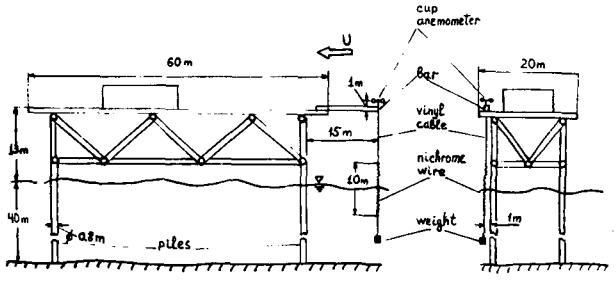

FIG. 1. A simplified sketch of the tower with the observational equipment.

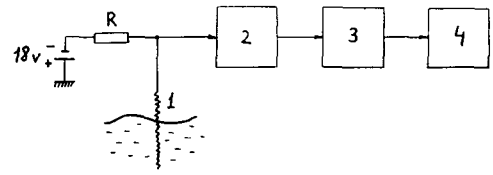

FIG. 2. Block-diagram of the measuring system: (1) probe, (2) digital voltmeter (type V-2-22), (3) code converter, (4) recorder.

The wave gauge was supported by a horizontal bar extending from the up-wind side of the platform and was located 15 m away from the nearest pile (Fig. 1). We have done no theoretical estimation of the possible effect on the wave measurement of reflections from piles and other supports of the platform. However our visual observations clearly showed the absence of any disturbances at the probe point, and there was no difference in the fine structure of the sea surface at the probe and at a distance from it. So we believe the distortions of the wave field at the probe produced by the platform to be negligibly small.

Waves were measured by a resistance-type wave gauge which is composed of a resistance probe of a single 0.3 mm diameter nichrome wire and an electronic circuit as shown in Fig. 2. The probe is inserted into a series direct current circuit ($J \approx 38$ ma). Such a scheme for resistance wire gauge was offered earlier by Konyaev (1969) and its suitability for wind waves measurements has been confirmed in our previous experiments (Leykin and Rozenberg, 1970).

The frequency response of the wire probe has proved to be approximately constant for wave frequencies up to 30 Hz (Mitsuyasu and Honda, 1974). It is important to note that measurements of the high-frequency part of the wind-wave spectra $S(\omega)$ are mainly limited not by the probe response but by the restricted dynamical range of the recording system, which usually amounts to not more than 30–40 dB.

In our previous measurements of high-frequency wind wave spectra (Leykin and Rozenberg, 1970) we used an amplifier with a special frequency response as a prewhitening device. The recorded signal spectra were then converted to wave spectra taking into account this frequency response. As a matter of fact, the same method was used by Mitsuyasu (1977).

In the present experiments we used a digital tape recorder system with large dynamical range. The simplified block diagram of this system is shown in Fig. 2. The probe signal passes to the electronic digital voltmeter 2 (type V-2-22) and is converted into parallel decimal code with a sampling frequency of 50 Hz. Then the parallel code is converted to sequential code by converter 3 and is recorded on tape recorder 4. This method of recording provided a dynamical range of about 83 dB. As the level of voltmeter self-noise is

less than 10^{-5} V, and the probe transfer coefficient is 5.3×10^{-3} V cm^{-1}, the wave gauge made it possible to measure with amplitude resolution 2.0×10^{-4} m in the presence of sea waves with height (from trough to crest) up to 4 m.

3. Wave observations and data analysis

Wave measurements were made in June–July 1978 for different wind and wave conditions. Cases studied in this paper represent situations with steady north winds, because under these conditions the fetch from the upwind shore to the measuring station was about 500 km. We have investigated only "classical" wind wave cases with no swell on the sea surface.

Wind mean speed U and its direction (for 5-min. intervals) were measured by a standard cup anemometer located at 14 m above the sea surface. These values of U are used below in the data analysis.

During the measurements the wave signal $\zeta(t)$ was recorded on a magnetic tape for 4–10 min. For spectral analysis we have used the samples of 3 min length consisting of 9000 data points with time interval 0.02 s. These data were used for estimating the autocorrelation function $R(\tau)$ and spectral density function $S(\omega)$. The statistical computations were made on a computer following the standard method (Jenkins and Watts, 1969) with a Bartlett function as a lag window.

The calculated spectral density function $S(\omega)$ satisfies the normalization condition,

$$\int_0^\infty S(\omega)d\omega = \sigma_H^2 = \langle \zeta^2 \rangle \qquad (3)$$

where σ_H^2 is the variance of surface displacements.

In order to evaluate the spectrum $S(\omega)$ for signals of large dynamical range we calculate separately the spectra for low-frequency (0–1 Hz), intermediate (1–2.5 Hz) and high-frequency (2–10 Hz) ranges of the spectrum $S(\omega)$ with preliminary elimination of the energy-containing components with help of the digital high-pass filter. We used a filter with the kernel

$$h_i = \frac{1}{q+1}\left[\frac{1}{2} + \frac{1}{2}\cos\left(\frac{\pi}{q+1} i\right)\right], \qquad (4)$$

where $i = -q, -q+1, \ldots, 0, 1, \cdots q$, q a parameter of the filter. The value of frequency resolution changed from 0.1 Hz in the low-frequency range to 0.4 Hz in the high-frequency range so the computed spectra had from 70 to 270 degrees of freedom respectively. Thus limits of the 95% confidence band of the measured spectrum $S(\omega)$ are approximately $0.73S(\omega)$ and $1.40S(\omega)$ for the low-frequency range and $0.80S(\omega)$ and $1.35S(\omega)$ for the high-frequency range.

It is important to take into account that the statistics of the short waves are related mainly to long wave components (see Section 5 of this paper), so it is necessary to evaluate high-frequency spectra $S(\omega)$ only for samples long enough with respect to the typical long wave period $T_m = 2\pi/\omega_m$, or else the estimated spectrum may not be reliable in spite of the large value of degrees of freedom. In the present measurements the wave record usually contained from 35 to 70 long wave periods T_m, so one can consider the evaluated high-frequency spectra $S(\omega)$ to be statistically reliable.

Typical examples of the wind wave spectra $S(\omega)$ obtained for different wind speeds are shown in Fig. 3. The method of measurements and data analysis made it possible to evaluate spectra $S(\omega)$ in the frequency range up to 10 Hz. Note that the values of spectral density vary over a range of 9 orders approximately.

4. Results

For the present analysis 20 spectra $S(\omega)$ were chosen, all of them corresponding to developing wind waves with mean wind speeds from 3.5 to 13.5 m s^{-1}. For every spectrum $S(\omega)$ the values of the frequency of the spectral peak ω_m, surface-displacement variance σ_H^2 [Eq. (3)] and orbital velocity variance

$$\sigma_v^2 = \int_0^\infty S(\omega)\omega^2 d\omega \qquad (5)$$

were determined. The values of the parameter c_m/U (where $c_m = g/\omega_m$ is the phase speed of the energy

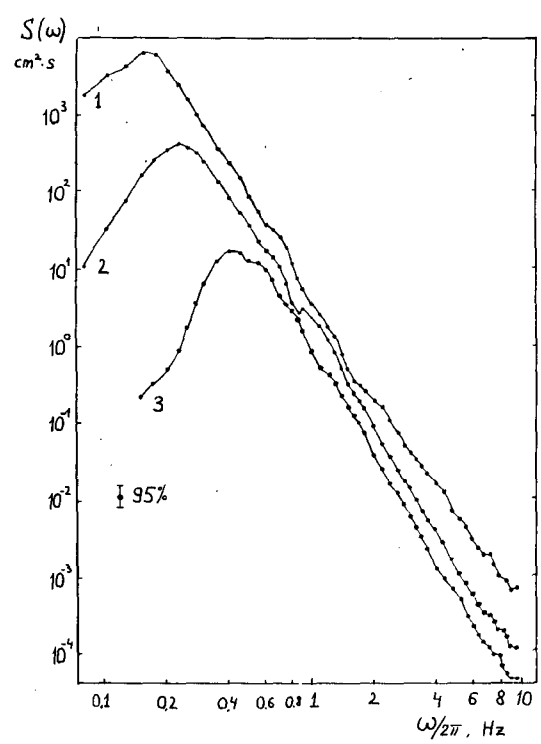

FIG. 3. Wind-wave frequency spectra $S(\omega)$ for different wind speeds: (1) U = 13.5 m s^{-1} (1.07.78 N 14), (2) U = 6 m s^{-1} (1.07.78 N 2), (3) U = 3.5 m s^{-1} (30.06.78 N 17).

containing components) characterizing the stage of the development of waves were also determined. The values of ω_m, σ_H^2, σ_v^2 and c_m/U are summarized in Table 1.

For most of the cases under consideration the values of c_m/U vary from 0.7 to 1 which correspond to nearly fully developed wind waves. For that case the values of σ_H^2 and σ_v^2 grow and the values of ω_m decrease with increasing wind speed. As an example the dependence of σ_H and ω_m on the wind speed U is shown in Fig. 4.

To determine the dependence of the spectral parameters on the stage of wave development all the spectra were divided into three groups with respect to the value of c_m/U ($c_m/U > 0.8$–9 spectra; $0.7 \leqslant c_m/U \leqslant 0.8$–6 spectra; $c_m/U < 0.7$–5 spectra). These groups of data are shown in Fig. 4, Figs. 6 and 7 by solid circles, crosses and open circles, respectively.

In order to investigate in detail the high-frequency range of the spectra $S(\omega)$ all the measured spectra have been normalized to the non-dimensional form

$$\tilde{S}(\omega) = S(\omega)\omega^5 g^{-2}. \quad (6)$$

In Fig. 5 our spectra $S(\omega)$ considered above (see Fig. 3) are shown in the form (6). Such a normalization displays the deviations of the measured spectra from Phillips' spectrum (1) which is also shown in Fig. 5 (horizontal line).

The data plotted in Fig. 5 indicate that there is a significant discrepancy between the observed spectra $S(\omega)$ and Phillips' spectrum Eq. (1)

1) The absolute values of spectral density systematically exceed the values calculated according to Eq. (1),

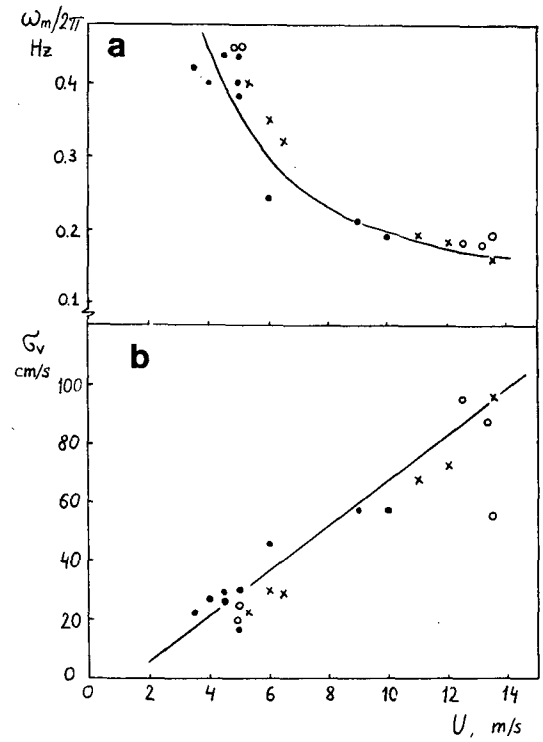

FIG. 4. (a) The change of the spectral-peak frequency ω_m and (b) rms value of the orbital velocity σ_v with the wind speed U: $c_m/U > 0.8$ (solid circles); $0.7 \leqslant c_m/U \leqslant 0.8$ (crosses) and $c_m/U < 0.7$ (open circles). Solid lines indicate the mean trend of the data.

2) Observational data display the growth of the spectral density at a fixed frequency S_{ω_i} with mean wind speed,

3) The shapes of measured spectra differ from the

TABLE 1. Wind wave parameters.

Number	Date	U (m s^{-1})	$\omega_m/2\pi$ (Hz)	c_m/U	σ_H^2 (cm^2)	σ_v^2 (cm^2 s^{-2})	α	n
1	25 June 1	12.0	0.18	0.72	2.41×10^3	5.30×10^3	3.54×10^2	3.39
2	3	12.5	0.18	0.69	3.63×10^3	8.96×10^3	1.93×10^2	3.21
3	27 June 1	5.0	0.45	0.69	4.10×10^2	6.00×10^2	2.00×10^3	4.24
4	2	4.0	0.40	0.98	5.90×10^2	7.34×10^2	8.73×10^3	4.78
5	28 June 3	5.0	0.45	0.69	2.38×10^1	3.81×10^2	1.22×10^2	3.37
6	29 June 1	5.0	0.38	0.82	4.10×10^1	5.50×10^2	6.92×10^3	4.62
7	2	4.5	0.38	0.91	7.30×10^1	8.62×10^2	8.40×10^2	3.97
8	3	6.5	0.32	0.75	1.05×10^2	8.15×10^2	8.60×10^2	4.05
9	5	6.0	0.35	0.74	9.15×10^1	8.72×10^2	7.90×10^2	3.95
10	9	5.3	0.40	0.74	4.05×10^1	4.93×10^2	1.52×10^3	4.26
11	30 June 10	5.0	0.38	0.82	8.92×10^1	8.65×10^2	1.01×10^3	4.10
12	15	4.5	0.40	0.87	6.04×10^1	6.40×10^2	1.26×10^4	4.82
13	17	3.5	0.42	1.06	3.72×10^1	5.02×10^2	4.23×10^3	4.59
14	1 July 2	6.0	0.24	1.08	4.83×10^2	2.10×10^3	6.10×10^3	4.44
15	4	9.0	0.21	0.82	1.02×10^3	3.33×10^3	4.90×10^2	3.46
16	7	10.0	0.19	0.82	1.01×10^3	3.30×10^3	2.95×10^3	4.19
17	8	11.0	0.19	0.75	1.73×10^3	4.61×10^3	2.20×10^3	3.91
18	10	13.5	0.19	0.61	1.22×10^3	3.03×10^3	6.19×10^2	3.67
19	13	13.3	0.18	0.65	3.85×10^3	7.68×10^3	1.10×10^3	3.55
20	14	13.5	0.16	0.72	5.48×10^3	9.20×10^3	2.16×10^3	3.69

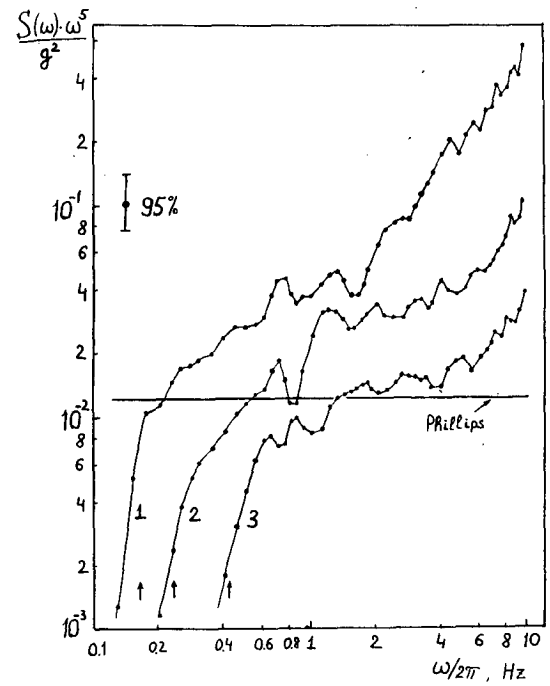

FIG. 5. Nondimensional spectra $\tilde{S}(\omega) = S(\omega)\omega^5 g^{-2}$. Arrows indicate the position of the spectral-peak frequency ω_m. For legend see Fig. 3.

ω^{-5} power law and are a more satisfactory fit to the ω^{-4} law.

These qualitative conclusions are in good agreement with the results of our previous measurements (Leykin and Rozenberg, 1970). The significant irregularity of spectra $S(\omega)$ in the frequency range $\omega/2\pi \geq 3$ Hz reported by Leykin and Rozenberg is possibly related to the measurement site (coastal zone) and has not been observed in the present investigation.

To investigate the high-frequency range of the measured spectra $S(\omega)$ more quantitatively the dependence of the values of the spectral density at a fixed frequency S_{ω_i} on the wind speed U has been examined first. Typical values of S_{ω_i} for several spectral components ($\omega_i/2\pi$ = 3, 4 and 6.4 Hz) are plotted in Fig. 6.

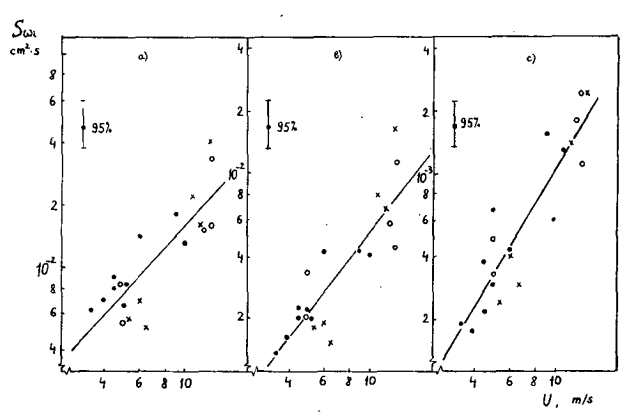

FIG. 6. Growth of the spectral density at a fixed frequency $S\omega_i$ with wind speed for the spectral components (a) 3 Hz, (b) 4 Hz and (c) 6.4 Hz. Solid lines indicate fit functions $S_{\omega_i} = \gamma U^m$ (Table 2). For symbols see Fig. 4.

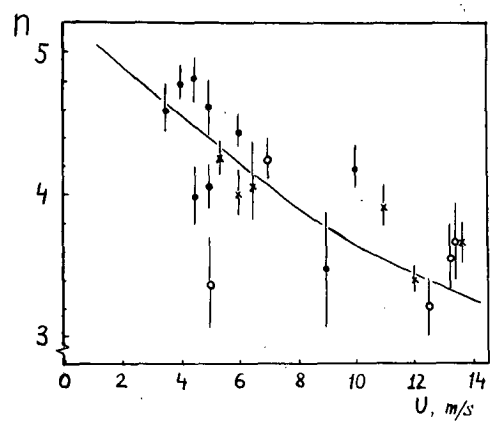

FIG. 7. The change of the shape parameter η with the wind speed. For symbols see Fig. 4.

The consideration of these and other spectral components clearly shows that within the frequency range 2–8.8 Hz all the spectral components grow in amplitude with the wind speed. It can be seen from Fig. 6 that the relation between S_{ω_i} and U can be approximately expressed by a power law $S_{\omega_i} = \gamma U^m$. Note that the scatter of the data in Fig. 6 increases for the less developed waves ($c_m/U \leq 0.7$).

The mean values of γ, m and also the 95% confidence limits of m were determined by the least squares method. The results are listed in Table 2. The values of m systematically increase from 0.85 to 1.70 as the frequency increases from 2 to 8.8 Hz: that is, the high-frequency components of wind waves have the highest growth rate.

In order to investigate the shape of the high-frequency range of the wind-wave spectrum we expressed all the measured spectra $S(\omega)$ by a power law $S(\omega) = \alpha\omega^{-n}$ within the frequency range from 2.4 to 7.2 Hz. The values of α and n were determined by the method of least squares and are listed in Table 1. In

TABLE 2. Mean values of γ and m including 95% confidence limits as determined by least squares method.

$\omega_i/2\pi$ (Hz)	γ	m
2.0	0.13×10^{-1}	0.85 ± 0.34
3.0	0.13×10^{-2}	1.09 ± 0.36
4.0	0.25×10^{-3}	1.32 ± 0.38
5.2	0.68×10^{-4}	1.46 ± 0.34
6.4	0.21×10^{-4}	1.71 ± 0.40
7.6	0.13×10^{-4}	1.62 ± 0.46
8.8	0.77×10^{-5}	1.70 ± 0.50

Fig. 7 the relation of shape parameter n to mean wind speed U is plotted. The data of Fig. 7 show that with the increase of wind speed the values of n systematically fall from 4.8 to 3.3. This result is consistent with the dependence of the rate of growth of spectral components with wind found for particular frequencies ω_i mentioned above. Note, that although this feature of wave spectra would not be expected to depend on the stage of development of waves, yet the scatter of values of n and also the limits of the 95% confidence band for n are somewhat greater for the less developed waves than for the rest of the data.

A scatter diagram showing the relation between the parameters n and α is plotted in Fig. 8. The data of Fig. 8 clearly show the linear relation between n and $\log\alpha$. The correlation coefficient between n and $\log\alpha$ was found to be 0.91 which exceeds the 95% significance level. A similar relationship between the shape parameter n and α was mentioned earlier by Grose *et al.* (1972).

It is necessary to take into account that the shape of the spectrum at high frequency can depend not only on wind speed but also on the parameters of energy-containing long-wave components. As was mentioned above (see Fig. 4), in the present measurements the parameters of energy-containing components systematically change with wind so that one cannot separate the influence of long waves and of wind on features of the high-frequency range of the spectrum.

A consideration of nondimensional spectra $\tilde{S}(\omega) = S(\omega)\omega^5 g^{-2}$ shows (see Fig. 5) that as the frequency

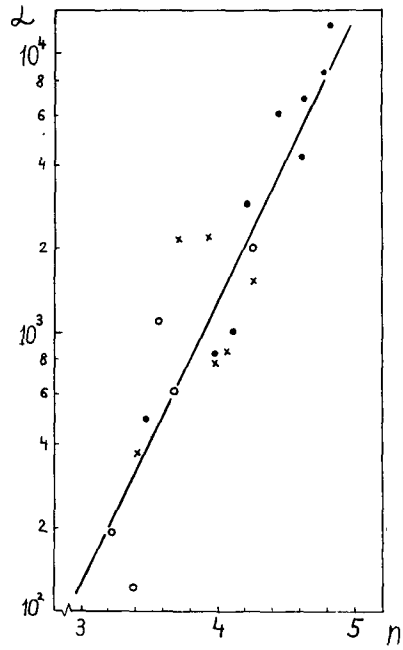

FIG. 8. Scatter diagram of the parameters α and η from fit function $S(\omega) = \alpha \cdot \omega^{-n}$. Solid line indicates fit function $\log\alpha = -0.92 + 1.01n$. For symbols see Fig. 4.

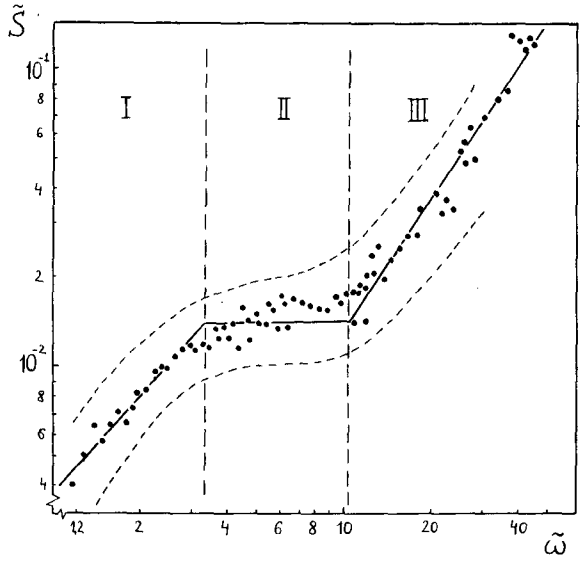

FIG. 9. The mean nondimensional spectrum $\tilde{S} = S(\omega)\omega^5 g^{-2}$ in relation to nondimensional frequency $\tilde{\omega} = \omega/\omega_m$. Solid lines are fit functions (7); dotted lines indicate rms deviation. I—the range near the spectral peak; II—equilibrium range; III—high-frequency range.

increases from the spectral-peak value ω_m the values of $\tilde{S}(\omega)$ first increase, then in a certain frequency range $\omega_1 < \omega < \omega_2$ level off and afterwards (for $\omega > \omega_2$) begin to increase again. One may assume that the shape of the spectrum $\tilde{S}(\omega)$ at high frequency depends on the difference in frequency from the spectral-peak value ω_m.

In order to verify this assumption all the nondimensional spectra $\tilde{S}(\omega)$ have been plotted against the nondimensional frequency $\tilde{\omega} = \omega/\omega_m$ and averaged. The mean spectrum based on 20 individual spectra is exhibited in Fig. 9. The data of Fig. 9 clearly show that the use of the nondimensional frequency $\tilde{\omega}$ provides an effective grouping of initial spectra. The values of rms deviation are shown by dotted line: they do not exceed 25% of the mean value in frequency range $\tilde{\omega} = 1.2$ to 30.

There still remains a weak dependence of the spectral density at a fixed frequency $\tilde{S}_{\tilde{\omega}_i}$ on the wind speed, but the values of $\tilde{S}_{\tilde{\omega}_i}$ change at most by a factor of 2 as the wind speed increases from 3.5 to 13.5 m s^{-1}. Note that this is a small change relative to the change of spectral density S_{ω_i} at the fixed absolute frequency ω_i (see Fig. 6 and Table 2).

In the mean spectrum $\tilde{S}(\tilde{\omega})$ shown in Fig. 9 one can conditionally distinguish three ranges

1) the frequency range near the spectral peak ($1.2 \leqslant \tilde{\omega} \leqslant 3.2$) where $\tilde{S}(\tilde{\omega}) \sim \tilde{\omega}^1$,

2) the equilibrium range ($3.2 \leqslant \tilde{\omega} \leqslant 10.5$) where $\tilde{S}(\tilde{\omega}) \approx$ constant,

3) the high-frequency range ($\tilde{\omega} > 10.5$) where $\tilde{S}(\tilde{\omega}) \sim \tilde{\omega}^{1.5}$.

If one neglects the weak dependence of the values of $\tilde{S}(\tilde{\omega})$ on the wind speed one may suggest the following empirical approximation for the nondimensional spectrum $\tilde{S}(\tilde{\omega})$

$$\tilde{S}(\tilde{\omega}) = \begin{cases} 4.0 \times 10^{-3}\,\tilde{\omega}^{1}, & 1.2 \leqslant \tilde{\omega} \leqslant 3.2 \\ 1.4 \times 10^{-2} = \text{constant}, & 3.2 \leqslant \tilde{\omega} \leqslant 10.5 \\ 4.5 \times 10^{-4}\,\tilde{\omega}^{1.5} & 10.5 \leqslant \tilde{\omega} \leqslant 30. \end{cases} \tag{7}$$

In Fig. 9 the approximative relations (7) are shown by solid lines. Note that the approximation (7) is expressed in terms of the difference of frequency from the spectral-peak frequency.

5. Discussion

The data obtained here as well as the results of previous investigations strongly confirm that there is no equilibrium range in the high-frequency part of the wind wave spectrum. Nevertheless there are some difficulties in interpreting these results.

First, one can note that such main features of the measured spectra as the dependence of spectral density at fixed frequency on the wind speed and the difference between the measured shapes of the spectra and Phillips' spectrum [Eq. (1)] are in good agreement with the universal relation obtained by Zakharov and Filonenko (1966) within the framework of the theory of weak turbulence. These authors assumed that the shape of the spectrum in the high-frequency range is governed by energy flux P from the range of input to the range of dissipation, and for the frequency spectrum of gravity waves they have obtained (Zakharov and Filonenko, 1966).

$$S(\omega) = P^{1/3}\omega^{-4}. \tag{8}$$

According to Barenblatt and Leykin (1981), spectrum (8) may be represented in a form

$$S(\omega) = \gamma_1 g u_* \omega^{-4}, \tag{8a}$$

(where γ_1 is a universal constant and u_* is air friction velocity) which discloses the dependence of the spectral density $S(\omega)$ on wind speed.

However the comparison of experimental data with the relation (8a) must be done with care. If one assumes that the dispersion relation for linear free gravity waves $\omega^2 = gk$ is valid for wind waves, then the expressions for frequency and wavenumber spectra obtained by Phillips (1958, 1977) and by Zakharov and Filonenko (1966) [for example, Eq. (1), (2)] are equally valid. Yet even within the framework of a standard potential model of weakly nonlinear surface waves the dispersion relation for the short wave components may be significantly distorted as a result of Doppler shift of the frequency by the orbital motion of long wave components (Sinitsyn *et al.*, 1973). Since the data available are frequency spectra $S(\omega)$, it may be that the observed deviations from Phillips' spectrum [Eq. (1)] can be related, at least partially, to the influence of long wave components.

A simplified model of this effect has been considered by Sinitsyn *et al.* (1973) within the framework of the "adiabatic" approximation which only accounts for the influence of the long waves on the short waves. They assumed that the short wave wavenumber spectrum $\psi(\mathbf{K})$ is described by Phillips' spectrum [Eq. (2)] and that its intensity does not depend on the location along the long wave. Calculations made by Sinitsyn *et al.* have shown that this model provides a spectral shape corresponding to the ω^{-4} power law, and that the absolute values of the spectral density at a fixed frequency grow with increase of the long wave orbital velocity. This result is in good agreement with the observational data in spite of the fact that the model does not take into account the variance of the intensity of short waves along the long wave due to different wave generation conditions. These "intermittent effects" (see Phillips, 1977) have been observed both in laboratory (Reece, 1978; Lee, 1977) and in field measurements (Plant *et al.*, 1978; Evans and Shemdin, 1980).

In an analogous way the spectra $S(\omega)$ can be distorted by the permanent current (Kitaigorodskii *et al.*, 1975), particularly by the wind-induced drift current. As the value of drift velocity near the surface, $v_0 \approx 3 \times 10^{-2} U$, is comparable to the phase speed of the short wave components and linearly related to wind speed U, this effect also can result in an increase of spectral density at a fixed frequency with an increase of wind speed.

What is more, the presence of a thin wind drift layer with high vorticity near the surface leads to breaking of short wave components (Banner and Phillips, 1974). As a result the high-frequency part of the spectrum $S(\omega)$ becomes dependent on wind speed, and in the general case Eq. (1) takes the form (Phillips, 1977)

$$S(\omega) = g^2\omega^{-5} f_1(\omega u_*/g), \tag{9}$$

where f_1 is an unknown function. For the frequency range $\omega \ll 2g/u_*$ the surface drift influence on the intensification of breaking of short wave components happens to be negligibly small (Phillips, 1977), and Eq. (9) reduces to Phillips' equilibrium spectrum Eq. (1). However the presence of long waves leads to a nonlinear increase of the surface drift near the long wave crests which is shown (Phillips and Banner, 1974) to reduce the maximum amplitude that the short waves can attain before breaking. This effect makes it rather difficult to evaluate the high-frequency spectrum parameters for real conditions (see discussion by Phillips, 1977).

Therefore the available data do not allow a definite conclusion on the cause of the observed relation between the high-frequency part of the spectrum $S(\omega)$ and the wind speed. In particular it is impossible to distinguish the real increase of ripple intensity, related, for example, to the direct transfer of energy from wind or to nonlinear wave–wave interactions, from the apparent increase of the values of $S(\omega)$ due to the Doppler

shift of the frequency of short waves, which is induced by the large-scale motions in the sub-surface layer.

Note that the understanding of microwave remote sensing of the sea surface needs information about the short-wave wavenumber spectrum $\psi(\mathbf{K})$ because in first-order scattering theory the microwave backscattering cross section per unit area σ_0 and spectral density $\psi(\mathbf{K})$ are proportional (Bass *et al.*, 1968). As there is no definite relation between the frequency spectrum $S(\omega)$ and the wavenumber spectrum $\psi(\mathbf{K})$ the use of the frequency spectra $S(\omega)$ for these purposes must be done with particular care.

Pierson and Stacy (1973) proposed a wavenumber spectrum $S(k)$[1] for fully developed ocean waves which ranges from the spectral-peak frequency to capillary ripples and consists of five regions. Particularly for the spectral range $k_2 = 0.359\ \text{cm}^{-1} \leqslant k \leqslant k_3 = 0.942\ \text{cm}^{-1}$ which corresponds to the frequency range $\omega/2\pi = 3.0$ to 5.0 Hz they proposed

$$S_3(k) = 4.05 \times 10^{-3} D(u_*) k_3^{-p} k^{-3+p}, \quad (10)$$

where

$$D(u_*) = (1.247 + 0.0268u_* + 6.03 \times 10^{-5} u_*^2)^2, \quad (11)$$

$$p = \log[D(u_*)/(u_*/u_{*m})]/\log(k_3/k_2), \quad (12)$$

and $u_{*m} = 12\ \text{cm s}^{-1}$. Spectrum (10), which they call the "Leykin–Rozenberg spectral range" was based on the high-frequency spectra of wind waves reported in our earlier paper (Leykin and Rozenberg, 1970). The measured frequency spectra $S(\omega)$ were transformed into the wavenumber spectra $S(k)$ by using the relation

$$S(k)dk = S(\omega)d\omega \quad (13)$$

and by assuming the dispersion relationship

$$\omega = \omega(k) = (gk + T_s/\rho_w \cdot k^3)^{1/2}, \quad (14)$$

where T_s is surface tension and ρ_w is the density of water.

The approximate formulas of Pierson and Stacy (1973), particularly Eq. (10), are now widely used for interpretation of the microwave backscattering data. Yet the above consideration clearly shows that the use of such simple relations [Eq. (13), (14)] for the high-frequency part of the wind-wave spectrum cannot be regarded as well established.

In order to describe satisfactorily the wind-wave frequency spectrum $S(\omega)$ within the range $\omega > \omega_m$ one must take into account both the effect on the short-wave wavenumber spectrum $\psi(\mathbf{K})$ of long waves and the modification of the short-wave dispersion relation by the large-scale motions in the sub-surface layer. These effects are not yet well understood. Under the assumption of incomplete self-similarity of the frequency spectrum of the wind waves on the dimensionless parameter $\omega U/g$, a self-similar spectrum has been obtained by Barenblatt and Leykin (1981) in the form

$$S(\omega) = g^2 \omega^{-5} (\omega U/g)^{\alpha_1} F_1, \quad (15)$$

where α_1 and F_1 are functions of the dimensionless parameter $g\lambda_m/U^2$ characterizing the stage of development of the waves (λ_m is the wavelength of the energy-containing components of the spectrum).

At the same time the existence of the universal spectrum $\tilde{S}(\tilde{\omega})$ [Eq. (7)] which describes rather satisfactorily all the observational spectra within the broad range of the nondimensional frequencies ($\tilde{\omega} = 1.2$–30) leads us to assume that, in order to understand the equilibrium range in the wind wave spectra $S(\omega)$, one must consider not the absolute frequency as is usual but the distance of a particular frequency from the spectral-peak frequency. Following this assumption we propose a new model for the frequency spectrum $S(\omega)$ for $\omega > \omega_m$ based on the observational data. It is possible to distinguish in the spectrum $S(\omega)$ three characteristic ranges

1) The range located near the spectrum maximum ($1.2 \leqslant \tilde{\omega} \leqslant 3.2$) where $S(\omega) \sim \omega^{-4}$. One may assume an active growth of the spectral components within this range.

2) The equilibrium range ($3.2 \leqslant \tilde{\omega} \leqslant 10.5$) where the spectrum $S(\omega)$ can be satisfactorily described by Phillips' spectrum Eq. (1) with $\beta = 1.4 \times 10^{-2}$.

3) The high-frequency range ($\tilde{\omega} > 10.5$) where $S(\omega) \sim \omega^{-3.5}$. The shape of the spectrum in this range is governed mainly by the orbital motion of the long wave components.

The physical meaning of the proposed model is the following: the equilibrium range, where the values of the spectral density $S(\omega)$ do not depend on the external parameters, migrates into the low-frequency part of the spectrum with the development of wind waves. If this is really so, one can explain the relation of the shape of the high-frequency range of the spectrum to the wind speed as observed in our measurements—the value of the spectral-peak frequency ω_m falls with increase in wind speed, and the fixed frequency range $2.4 \leqslant \omega/2\pi \leqslant 7.2$, which has been chosen for approximation by the power law, shifts along the universal curve (Fig. 9) into the region with smaller values of n. In an analogous way one can apparently explain the scatter of the values of n obtained by Yefimov and Kushnir (1974) who chose different ranges for the approximation of the spectrum $S(\omega)$.

Recently Zakharov and Zaslavskii (1983) showed that for sufficiently well developed wind waves the shape of the spectrum in the energy-containing range is defined by dimensional considerations of the transfer equation for wind waves where Kolmogorov's spectrum with respect to wave-action flux q is realised. They obtained

[1] Spectrum $S(k)$ represents the distribution of σ_H^2 over wavenumber regardless of direction and is related to the spectrum $\psi(\mathbf{K})$ as follows

$$S(k) = \int_0^{2\pi} \psi(\mathbf{K}) d\theta.$$

$$S(\omega) = aq^{1/3}g^{4/3}\omega^{-11/3}\theta_s(\omega/\omega_m), \qquad (16)$$

where a is a non-dimensional coefficient depending on the angular energy distribution for $\omega > \omega_m$, θ_s is a distributed Heaviside function cutting the spectrum at the spectral-peak frequency ω_m. The energy-containing range of the spectrum is not within the scope of this paper, but note that the shape of the spectrum, ω^{-4}, observed in our measurements for this range ($\tilde{\omega} \approx 1.2$–$3.2$) is very close to the shape $\omega^{-11/3}$ that is predicted by Eq. (16).

6. Conclusions

1) High-frequency spectra of wind generated waves were measured at a research tower in the Caspian Sea. A digital tape recorder system with dynamical range of about 83 dB made it possible to record spectra $S(\omega)$ within the frequency range up to 10 Hz.

2) The data obtained for nearly fully developed waves, corresponding to wind speeds from 3.5 to 13.5 m s^{-1} at 14-m elevation, clearly show that there is no equilibrium range in the high-frequency part of the wind-wave spectrum. The shapes of the measured spectra within the frequency range from 2.4 to 7.2 Hz differ from that predicted by Phillips' ω^{-5} power law and fit a law of the form, $S(\omega) \sim \omega^{-n}$, with the values of n varying from 3.2 to 4.8. The values of the spectral density at the fixed frequency S_{ω_i} where shown to grow significantly with the wind speed.

3) The observational data do not allow us to make a definite conclusion concerning the origin of the observed relation between the high-frequency part of the spectrum $S(\omega)$ and the wind speed. In particular, it is impossible to distinguish the real increase of ripple intensity from the apparent increase due to the Doppler shift of the frequency of short waves induced by the large-scale motions in the sub-surface layer.

4) Consideration of non-dimensional spectra $\tilde{S} = S(\omega)\omega^5 g^{-2}$ plotted versus nondimensional frequency $\tilde{\omega} = \omega/\omega_m$ leads us to assume that the equilibrium range in the wind-wave spectra does not exist in a fixed frequency range but migrates into the low-frequency part of the spectrum with the development of wind waves. A new model is proposed for the frequency spectrum $S(\omega)$ for $\omega > \omega_m$ based on the observational data in terms of the frequency difference between the range under consideration and the spectral-peak frequency.

Acknowledgment. We are indebted to V. I. Menshikov for his assistance in the spectral analysis of the wave data.

REFERENCES

Banner, M. L., and O. M. Phillips, 1974: On the incipient breaking of small scale waves. *J. Fluid Mech.*, **65**, 647–656.

Barenblatt, G. I., and I. A. Leykin, 1981: On the self-similar spectra of wind waves in the high-frequency range. *Izv. Akad. Nauk, SSSR, Fiz. Atmos. Okeana,* **17**, 50–58.

Bass, F. G., and collaborators, 1968: Very high frequency radiowave scattering by a disturbed sea surface: Pt. I, II. *Trans. IEEE,* **AP-16**, 5.

Evans, D. D., and O. H. Shemdin, 1980: An investigation of the modulation of capillary and short gravity waves in the open ocean. *J. Geophys. Res.*, **C85**, 5019–5024.

Grose, P. L., K. L. Warsh and M. Garstang, 1972: Dispersion relations and wave shapes. *J. Geophys. Res.*, **77**, 3902–3905.

Hasselmann, K., and collaborators, 1973: Measurements of wind-wave growth and swell decay during the Joint North Sea Wave Project (JONSWAP). *Dtsch. Hydrogr. Z.*, **12**, 1–95.

Jenkins, G. M., and G. J. Watts, 1969: Spectral analysis and its applications. Holden-Day, 596 pp.

Kitaigorodskii, S. A., V. P. Krasitskii and M. M. Zaslavskii, 1975: On Phillips' theory of equilibrium range in the spectra of wind-generated gravity waves. *J. Phys. Oceanogr.*, **5**, 410–420.

Kondo, J., Y. Fujinawa and G. Naito, 1973: High-frequency components of ocean waves and their relation to the aerodynamic roughness. *J. Phys. Oceanogr.*, **3**, 197–202.

Konyaev, K. V., 1969: The feeding of the string wave recorder by the direct current. *Izv. Akad. Nauk, SSSR, Fiz. Atmos. Okeana,* **5**, 216–217.

Lee, P., 1977: Doppler measurements of the effects of gravity waves on wind-generated ripples. *J. Fluid Mech.*, **81**, (Part 2), 225–240.

Leykin, I. A., and A. D. Rozenberg, 1970: Measurement of the high-frequency spectra of sea waves. *Izv. Akad. Nauk, SSSR, Fiz. Atmos. Okeana,* **6**, 1328–1332.

Mitsuyasu, H., 1977: Measurement of the high-frequency spectrum of ocean surface waves. *J. Phys. Oceanogr.*, **7**, 882–891.

——, and T. Honda, 1974: The high-frequency spectrum of wind-generated waves. *J. Oceanogr. Soc. Japan,* **30**, 185–198.

Phillips, O. M., 1958: The equilibrium range in the spectrum of wind-generated waves. *J. Fluid Mech.*, **4**, 426–434.

——, 1977: *The Dynamics of the Upper Ocean,* 2nd ed., Cambridge University Press, 336 pp.

——, and M. L. Banner, 1974: Wave breaking in the presence of wind drift and swell. *J. Fluid Mech.*, **66**, 625–640.

Pierson, W. J., and R. A. Stacy, 1973: The elevation, slope and curvature spectra of wind roughened sea surface. NASA Contractor Rep. CR-2247, 128.

Plant, W. J., W. C. Keller and J. W. Wright, 1978: Modulation of coherent microwave backscatter by shoaling waves. *J. Geophys. Res.*, **C83**, 1347–1352.

Reece, A. M., 1978: Modulation of short waves by long waves. *Bound.-Layer Meteor.*, **13**, 203–214.

Sinitsyn, Yu. A., I. A. Leykin and A. D. Rozenberg, 1973: On space-time characteristics of the ripple superimposed on long waves. *Izv. Akad. Nauk SSSR, Fiz. Atmos. Okeana,* **9**, 511–519.

Toba, Y., 1973: Local balance in the air–sea boundary process, III. *J. Oceanogr. Soc. Japan,* **29**, 209–225.

Yefimov, V. V., and V. M. Kushnir, 1974: Analysis of the high-frequency part of the sea waves' spectrum. *Oceanologia,* **14**, 30–36.

Zakharov, V. E., and Filonenko, 1966: Energy spectrum for stochastic oscillations of the surface of a liquid. *Dokl. Akad. Nauk SSSR,* **170**, 1292–1295.

——, and M. M. Zaslavskii, 1983: The shape of the spectrum of energy containing components of the water surface in the weakly turbulent theory of wind waves. *Izv. Akad. Nauk SSSR, Fiz. Atmos. Okeana,* **19**, 282–291.

Zaslavskii, M. M., and S. A. Kitaigorodskii, 1972: Intermittent pattern effects in the equilibrium range of the growing wind-generated sea. *Izv. Akad. Nauk SSST, Fiz. Atmos. Okeana,* **5**, 1230–1234.

Zubkovsky, S. L., O. A. Kuznetsov and G. N. Panin, 1974: Measurements of temperature, humidity and wind velocity fluctuations above the sea surface. *Izv. Akad. Nauk SSSR, Fiz. Atmos. Okeana,* **10**, 655–660.